The Formation of Metal (M=Co(II), Ni(II), and Cu(II)) Complexes by Aminosilanes Immobilized within Mesoporous Molecular Sieves

Dong Ho Park,[*] **Sung Soo Park, and Sang Joon Choe**

Department of Chemistry, Inje University, Kimhae, Kyongnam 621-749, Korea
Received November 21, 1998

The immobilization of APTMS(3-(2-aminoethylamino)propyltrimethoxysilane) and AAPTMS(3-(2-(2-aminoethyl)aminoethylamino)propyltrimethoxysilane) on the surface of high quality mesoporous molecular sieves MCM-41 and MCM-48 have been confirmed by F.T.-IR spectroscopy, Raman spectroscopy, ^{29}Si solid state NMR, and a surface polarity measurement using Reichardt's dye. The formation of metal (Co(II), Ni(II), and Cu(II)) complexes by immobilized aminosilanes have been investigated by photoacoustic spectroscopy(PAS). The assignment of UV-Vis. PAS bands makes it possible to identify the structure of metal complexes within mesoporous molecular sieves. Co(II) ion may be coordinated mainly in a tetrahedral symmetry by two APTMS onto MCM-41, and in an octahedral one by two AAPTMS. Both Ni(II) and Cu(II) coordinated by aminosilanes within MCM-41 form possibly the octahedral complexes such as $[Ni(APTMS)_2(H_2O)_2]^{2+}$, $[Ni(AAPTMS)_2]^{2+}$, $[Cu(APTMS)_2(H_2O)_2]^{2+}$, and $[Cu(AAPTMS)(H_2O)_3]^{2+}$, respectively. The PAS band shapes of complexes onto MCM-48 are similar to those of corresponding MCM-41 with the variation of PAS intensity. Most of metal ion(II) within MCM-41 and MCM-48 are coordinated by aminosilanes without the impregnation on the surface.

Introduction

The preparation and its potential applicability of the functionalized mesoporous silica surface have attracted considerable interest in recent years. Mesoporous molecular sieves, which was synthesized by Mobil group in 1992,[1,2] have a space enough to provide new heterogeneous catalytic environment within regular mesopores and the silanol group consisting of significant portion of surface.[2~4] MCM-41 exhibits a hexagonal array of one-dimensional mesopores, whose diameter was tuned from 15 to 100. Another mesoporous molecular sieve MCM-48 of cubic array which have a higher catalytic activity than MCM-41 consists of three-dimensional bicontinuous channels. However, the reports on MCM-48 are limited compared with MCM-41, probably due to the difficulty of its synthesis.

The chemical modification of mesoporous materials by anchoring of organometallic complexes to their surface of MCM-41 and MCM-48 with well ordered channels, unlike mesoporous silicas and acid treated clays, is an important area of research in heterogeneous catalysis and green chemistry. Liu *et al.* reported the alkene oxidation by ruthenium porphyrin encapsulated MCM-41,[5] Rao *et al.* achieved the immobilization of triazacyclononane ligands on a glyciated surface,[6] and O'Brien *et al.* could modify the surface of MCM-41 *via* ring opening of a ferrocenophane.[7] It is expected that the channel of mesoporous molecular sieves can be modified to a nanometer-sized reactor with specific function and shape by anchoring of transition metal complexes on the wall.

In the present work, we elucidate the immobilization of aminosilanes (3-(2-aminoethylamino)propyltrimethoxysilane (APTMS, $(CH_3O)_3Si(CH_2)_3NHCH_2CH_2NH_2$, 97%, Aldrich) and 3-(2-(2-aminoethyl)aminoethylamino)propyltrimethoxysiane ($AAPTMS$, $(CH_3O)_3Si(CH_2)_3NHCH_2CH_2NHCH_2CH_2NH_2$, tech, Aldrich)) within the mesopore of high quality MCM-41 and MCM-48 and the characteristics of the metal (Co(II), Cu(II), and Ni(II)) complexes formed by the immobilized aminosilanes using UV-Vis photoacoustic spectroscopy.

Experimental Section

The chemicals used in the synthesis were fumed silica (99.8%, metal-free, Sigma), cetyltrimethylammonium bromide (CTABr, 99%, Aldrich) and tetramethylammonium hydroxide (TMAOH, 25 wt% aqueous solution, Aldrich). Purely siliceous MCM-41 was synthesized following a literature procedure.[8] The molar composition of final gel mixture was 1.0 SiO_2 : 0.27 CTABr : 0.19 TMAOH : 40 H_2O. Purely siliceous MCM-48 was synthesized following literature procedure.[9] The sodium silicate solution was prepared using colloidal silica (Ludox HS40 (39.5 wt% SiO_2, 0.4 wt% Na_2O, and 60.1 wt% H_2O), Aldrich) added to the heated NaOH solution, whose molar composition is 0.25 Na_2O : 1.0 SiO_2 : 12.5 H_2O. This solution was added into the autoclave containing the surfactant solution of a mixture of CTABr, ethanol, and H_2O. The molar composition of resultant gel mixture is 1.4 SiO_2 : 1.0 CTABr : 0.35 Na_2O : 5.0 EtOH : 140 H_2O. The mixture was heated for 16 h at 413 K. After additional treatment for improvement of hydrothermal stability with NaCl solution, the product was then slurried in an ethanol-HCl mixture (0.1 mol of HCl per L of ethanol), filtered, washed with ethanol, dried in an oven, and calcined in air at 550 °C for 8 h.

The quality of MCM-41 and MCM-48 was confirmed by X-ray diffraction pattern and N_2 sorption measurement.

XRD patterns were recorded using a Philips 1710 powder diffractometer with Cu K_α radiation (40 kV, 40 mA), 0.02° step size and 1 s step time. N_2 adsorption isotherms were measured at -196 °C using a gas sorption analyzer (Quantachrome Corp., Nova-2000). The calculation of the pore size distribution (PSD) was performed using the Barrett-Joyner-Halenda (BJH) formula.[10] The cumulative surface area of the mesopores were obtained from PSD curves.

The procedure for immobilization of aminosilanes (ATPMS and AAPTMS) was as follows : MCM-41(0.1 g) degassed at 300 °C for 12 h in a vacuum (*ca.* 10^{-3} torr.) was saturated with a dry chloroform. The samples were stirred in a dry chloroform solution of aminosilanes (10 mL, 0.1 M) at room temperature for 12 h. After stirring, the samples were filtered and washed with chloroform and dichloromethane (1 : 1 (v/v)), dried at 40 °C for 12 h, and placed in an oven at 80 °C for 12 h to complete Si-O-Si formation, which were designated by APTMS/MCM-41 and AAPTMS/MCM-41, respectively. IR spectra were recorded on FT-IR spectrometer (Shimadzu Corp. FTIR-8201PC) with 2 cm^{-1} resolution and 100 scan times using the KBr pellet technique.

The APTMS/MCM-41 and AAPTMS/MCM-41 were immersed in a aqueous solution of 0.04 M-Co(CH₃CO₂)₂· 4H₂O, NiCl₂, and CuCl₂·2H₂O at room temperature for 2 h, respectively. The samples were filtered and washed with a deionized water, and dried at 80 °C for 12 h, which were design-ated by M(=Co(II), Ni(II), and Cu(II))/APTMS/MCM-41 and M/AAPTMS/ MCM-41.

According to Rosencwaig-Gersho theory for the photoacoustic effect,[11] the acoustic signal in optically opaque and thermally thick solids is proportional to the optical absorption coefficient of the solid sample for the wavelength and varies as (the chopping frequency)$^{-3/2}$. PAS technique made it possible to detect quantitatively the metal complexes coordinated by aminosilanes immobilized on the wall of MCM-41. PAS spectra were obtained using a home-made photoacoustic spectrometer as illustrated in other literature.[12]

^{29}Si MAS NMR spectra were recorded at 7.05 T using a Varian Unity Plus 300 spectrometer with zirconia rotors 7.5 mm in diameter spun in air at 5 kHz. Spectra were acquired at 59.6 MHz with 90° pulses and 600 s recycle delays. Chemical shifts are given in ppm from external tetramethylsilane (TMS).

In order to demonstrate the immobilization of aminosilanes, Raman spectrometer (Bruker Analytische Messtechnik GMBH) with InGaAs detector has been also used.

Results and Discussion

The quality of MCM-41 and MCM-48 was confirmed by XRD and N_2 sorption measurement. The XRD pattern of MCM-41 (Figure 1(a)) reflects the high quality of the crystallites. The (100) peak is sharp and intensive. The (110) and (200) peaks are well resolved, and the (300) peak is observed clearly. The calcined MCM-41 has a d₁₀₀ value of 44.4 Å, a pore diameter of 32.5 Å, and a surface area of 1185 m²/g (Figure 2). The XRD pattern of MCM-48 (Figure 1(b))
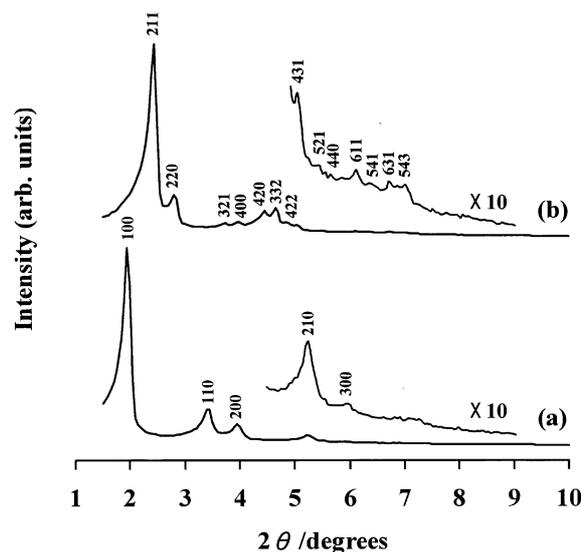
Figure 1. XRD patterns of (a) calcined MCM-41 and (b) calcined MCM-48.

shows typical peaks of the cubic crystallographic space group *Ia3d,* which indicates that the crystallites are particularly well-developed. The calcined MCM-48 has a pore diameter of 26.4 Å and a surface area of 972 m²/g as shown in Figure 2.

Figure 3 shows the IR spectra of (a) calcined MCM-41, (b) APTMS/MCM-41, and (c) AAPTMS/MCM-41. As compared with the IR spectra of calcined MCM-41 (Figure 3(a)), some characteristic peaks for the immobilization of aminosilanes appeared as denoted by solid circle in Figure 3(b) and 3(c). Both 2870 cm^{-1} and 2960 cm^{-1} for aliphatic CH stretching, 1558 cm^{-1} for NH scissoring, 1473 cm^{-1} for CH_2 bending and 1329 cm^{-1} for CH_3 bending can be assigned. The 960 cm^{-1} peak for silanol group of MCM-41 was weakened possibly due to the formation of Si-O-Si linkage between aminosilane and MCM-41 with demethanoliza-
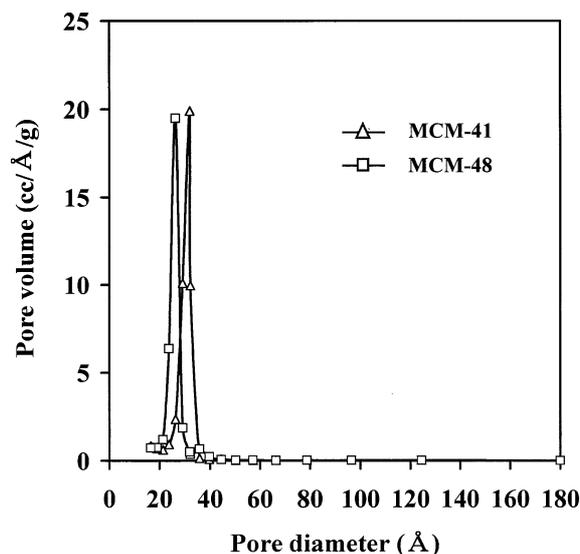
Figure 2. Pore size distribution curves of calcined MCM-41 and calcined MCM-48 calculated from the desorption branch of the nitrogen adsorption isothem using the BJH formula.
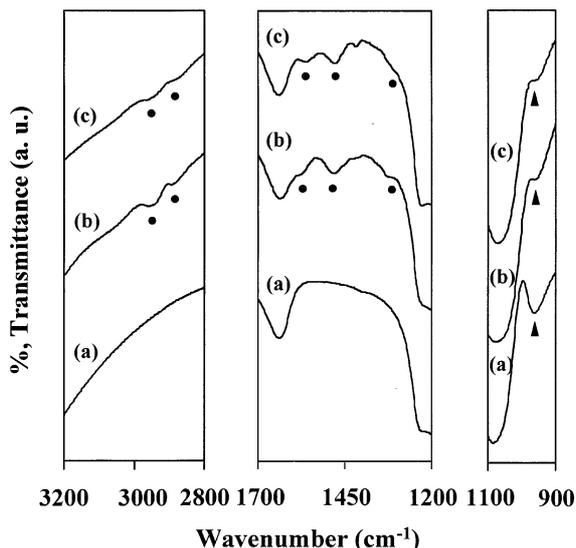
Figure 3. IR spectra of (a) calcined MCM-41, (b) APTMS/MCM-41, and (c) AAPTMS/MCM-41.

tion. The presence of CH_3 bending peak associated with 1329 cm^{-1} shoulder in Figure 3(b) and 3(c) indicates that all the methoxy groups in aminosilane do not participate the Si-O-Si linkage with surface silanol group of MCM-41. Chen et al. reported that there are at least four distinguishable types of silanol groups in MCM-41.[13] Depending on the local environment of silanol group, all or part of methoxy groups in aminosilane could be removed by the linkage formation.

There is no peak in Raman spectrum of calcined MCM-41 resulting from the amorphous silica wall (Figure 4(a)). On the other hand, the characteristic peaks of aminosilanes, except of the peaks in the spectra of APTMS and AAPTMS which are denoted by triangle (Figure 4(c) and 4(e)), have appeared on treatment of MCM-41 with aminosilane solutions (Figure 4(b) and 4(d)), indicating that aminosilanes
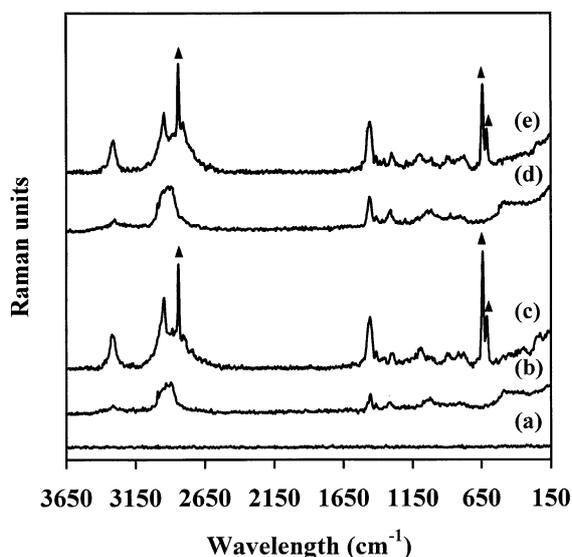

Figure 4. Raman spectra of (a) calcined MCM-41, (b) APTMS/MCM-41, (c) APTMS, (d) AAPTMS/MCM-41, and (e) AAPTMS.
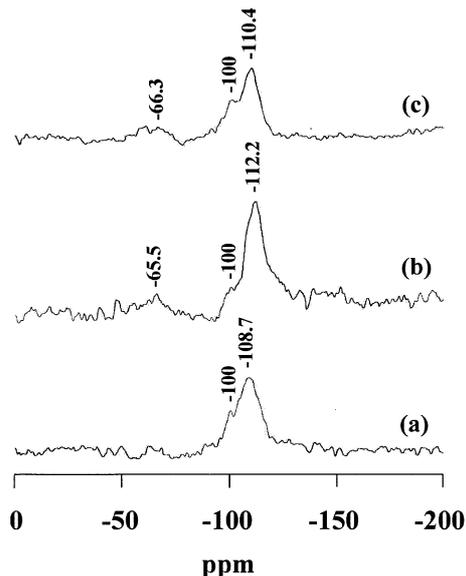

Figure 5. ^{29}Si MAS NMR spectra of (a) MCM-41, (b) APTMS/MCM-41, and (c) AAPTMS/MCM-41.

immobilized on the surface of MCM-41. The disappeared 2839 cm^{-1} peak could be assigned to C-H stretching mode of aminosilane's CH_3 removed during demethanolization.

The immobilization of aminosilanes is further confirmed by ^{29}Si MAS NMR spectra. Figure 5 shows ^{29}Si MAS NMR of (a) Si-MCM-41, (b) APTMS/MCM-41, and (c) AAPTMS/MCM-41, respectively. Peaks in the -100 ppm region are due to framework silicon atoms, with peaks at -100 ppm and -110 ppm for $Si(OSi)_3(OH)(Q_3)$ and $Si(OSi)_4(Q_4)$ structural units, respectively. The Q_3 peaks of APTMS/MCM-41, and AAPTMS/MCM-41 are weakened with appearance of peaks at *ca.* -66 ppm, indicating that part of the surface hydroxyl groups react with methoxy groups of aminosilanes. Peaks at -65.5 ppm and -66.3 ppm in the spectra of modified MCM-41 by aminosilanes are assigned to tridentate species which is the aminosilane bound to triple surface hydroxyl groups, as reported by De Haan *et al.*. The peak corresponding to bidentate species of *ca.* 59 ppm is not clearly absent.

Another evidence for the immobilization of aminosilane is the change of surface polarity of MCM-41. Reichardt's dye is a useful indicator of surface polarity of silica and alumina.[14,15] It is strongly solvatochromic and shows a range of energies for its $\pi \rightarrow \pi^*$ absorption band depending on the polarity of modified surface. The band of 700 nm range for Si-MCM-41 treated with Reichardt's dye solution reflects the hydrophobicity of MCM-41's surface, as shown in Figure 6(a). Upon treatment of Reichardt's dye for APTMS/MCM-41, λ_{max} was blue-shifted to 500 nm, which is due to organic group of APTMS bound on the surface of MCM-41. In case of AAPTMS/MCM-41, only weak band of 700 nm was occurred. It may be attributable that it is difficult for Reichardt's dye to diffuse into mesopores of MCM-41 due to blocking of long organic chain of AAPTMS anchored on the surface of MCM-41.

Figure 7 shows the photoacoustic spectra of (a) APTMS/MCM-41, (b) Co/APTMS/MCM-41, and (c) Co/AAPTMS/

294   *Bull. Korean Chem. Soc.* **1999**, Vol. 20, No. 3
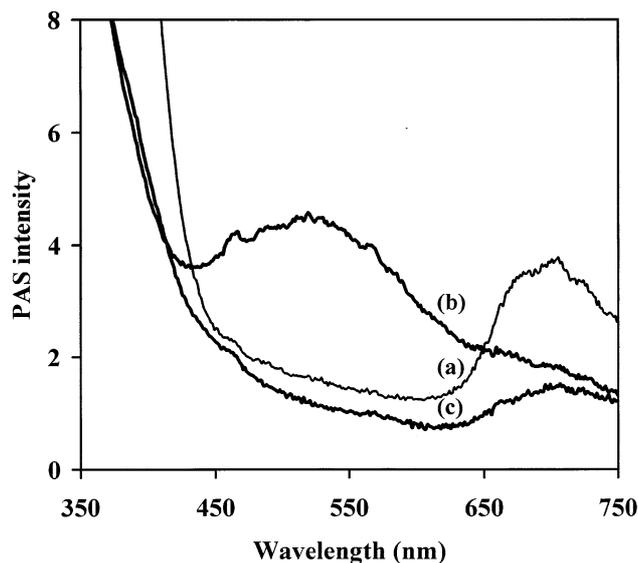
Dong Ho Park et al.

Figure 6. Photoacoustic spectra of (a) calcined MCM-41, (b) APTMS/MCM-41, and (c) AAPTMS/MCM-41 treated at room temperature for 1 h with Reichardt's dye solution (10 mL, 10^{-4} M), respectively.

MCM-41. Figure 7(a) shows the PAS spectrum of APTMS/MCM-41. There is no absorption band in this wavelength range. After treatment with Co(II) solution, the triplet bands around 600 nm and very intensive charge transfer band below 400 nm appeared as shown in Figure 7(b). In a crystal field environment of T_d symmetry, the ground-state energy level ^4F of Co(II) is split into three level, $^4A_2$, $^4T_2$, and $^4T_1(F)$, respectively.[16] Electronic transition among these and the next higher level $^4T_1(P)$ in a same spin state is allowed according to the selection rule for the electronic transition. The band due to the transition $^4T_1(P) \leftarrow {}^4A_2$ occurs in the range of visible and is split into triplet bands due to spin-

orbit coupling. Therefore, the triplet band around 600 nm can be responsible for the Co(II) complex coordinated tetrahedrally by two APTMS/MCM-41. Scheme 1(a) shows Co(II) coordinated by four ligating N atoms of two neighboring immobilized APTMS. Especially, λ_{max} values for triplet bands deconvoluted by curve-fitting calculation are 512 nm, 579 nm, and 650 nm, respectively, at almost same space (an inset in Figure 7), which is attributable to high tetrahedral symmetry of Co(II) complex. However, it is difficult to rule out completely the presence of Co(II) in octahedral environment since the intensity of the corresponding bands will be an order of magnitude lower and hence will be masked by the intense bands of the tetrahedral Co(II). In the case of Co/AAPTMS/MCM-41, PAS spectrum (Figure 7(c)) characteristic of octahedral structure, as shown in scheme 1(b), was obtained. It is attributable to coordination of Co(II) by six ligating N atoms of two neighboring immobilized AAPTMS. The band around 500 nm is a characteristic one for the octahedral complex $[Co(H_2O)_6]^{2+}$.[17,18] The weak band around 650 nm due to some tetrahedral structure, which is possibly related to Co(II) coordinated by the single AAPTMS, was showed.

Another evidence for the oxidation state of cobalt ion was obtained using VG Microtech. MT500 model electron spectrometer with X-ray excitation from MgK_α. Figure 8 illustrates the XPS spectra of Co/APTMS/MCM-41 and Co/AAPTMS/MCM-41. Smoothed curves of spectra in Co 2p energy region as shown in an inset in Figure 8 have satellite peaks on high binding energy side of $2p_{1/2}$ and $2p_{3/2}$ peaks, even though some obscurity due to low signal/noise ratio. Frost *et al.* have reported that Co(II) complexes have satellite peaks while low spin Co(III) complexes do not.[19]

Figure 9(a) and 9(b) show PAS's of Ni/APTMS/MCM-41, Ni/AAPTMS/MCM-41, respectively. Three spin-allowed transition are expected from the energy level diagram for Ni(II)
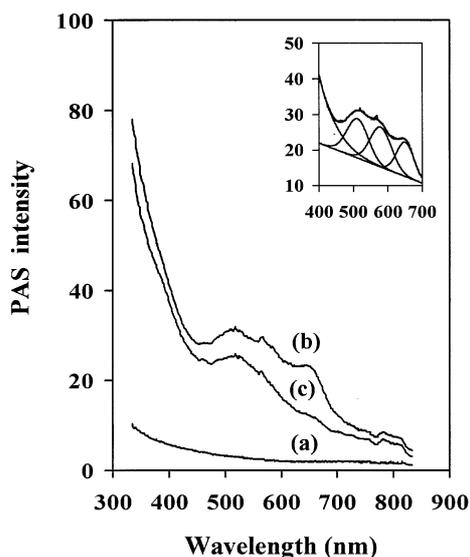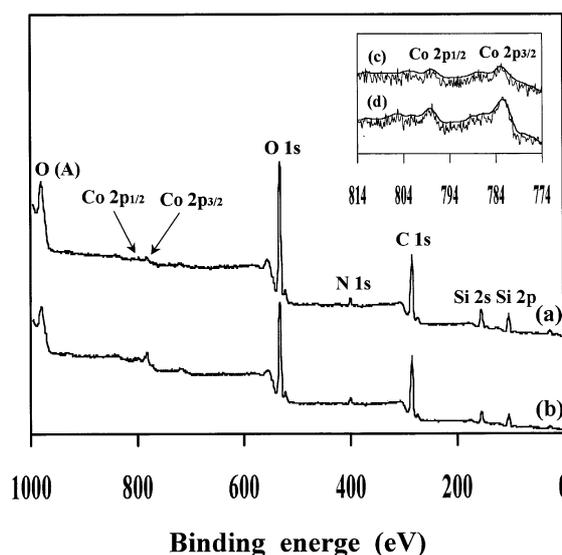

Figure 7. Photoacoustic spectra of (a) APTMS/MCM-41, (b) Co/APTMS/MCM-41, and (c) Co/AAPTMS/MCM-41. Inset shows the deconvoluted curves of PAS for Co/APTMS/MCM-41 by curve-fitting calculation.

Figure 8. X-ray photoelectron spectra of (a) Co/APTMS/MCM-41 and (b) Co/AAPTMS/MCM-41. Inset shows the smoothed and enlarged XP spectra of the cobalt 2p photoelectron region of (c) spectrum (a) and (d) spectrum (b).
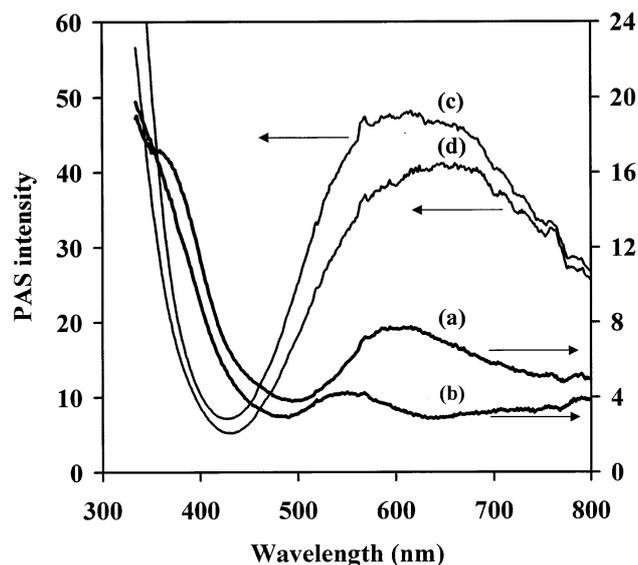
Figure 9. Photoacoustic spectra of (a) Ni/APTMS/MCM-41, (b) Ni/AAPTMS/MCM-41, (c) Cu/APTMS/MCM-41, and (d) Cu/AAPTMS/MCM-41.

Table 1. The atomic ratios of silicon to metal(Co, Cu, and Ni) ion using EDX

sample	Si/Co	Si/Cu	Si/Ni
Co/APTMS/MCM-41	35.2		
Co/AAPTMS/MCM-41	33.0		
Co/APTMS/MCM-48	36.4		
Co/AAPTMS/MCM-48	22.4		
Cu/APTMS/MCM-41		16.9	
Cu/AAPTMS/MCM-41		17.0	
Cu/APTMS/MCM-48		13.8	
Cu/AAPTMS/MCM-48		10.2	
Ni/APTMS/MCM-41			32.8
Ni/AAPTMS/MCM-41			28.7
Ni/APTMS/MCM-48			27.2
Ni/AAPTMS/MCM-48			19.6

ions in an octahedral complex, as reported in Ref(20). Two observed bands in PAS of Ni/APTMS/MCM-41 at λ_{max} of 380 nm and 600 nm can be assigned as the transitions corresponding to $^3A_{2g} \rightarrow ^3T_{1g}(P)$ and $^3A_{2g} \rightarrow ^3T_{1g}(F)$ for octahedral Ni(II) complexes, respectively.[20] It seems that Ni(II) is coordinated by two aminosilanes and two water molecules. The band for $^3A_{2g} \rightarrow ^3T_{2g}$ transition at a higher wavelength range can not be observed due to the limitation of light source for PAS. In case of Ni/AAPTMS/MCM-41, though the value of λ_{max} for $^3A_{2g} \rightarrow ^3T_{1g}(P)$ is not clear, both bands are blue-shifted comparing to those of Ni/APTMS/MCM-41, which may be due to the coordination with six ligating nitrogen atoms lying toward the stroger end of spectrochemical series than ligating oxygen atom of water. Both Ni(II) complexes coordinated by aminosilanes anchored to MCM-41 have an octahedral geometry. The PAS intensity of Ni/APTMS/MCM-41 is higher than that of Ni/AAPTMS/MCM-41, which is attributable to the increased molar absorptivity resulted from a lower symmetry of octahedral coordination sphere of $[Ni(APTMS)_2(H_2O)_2]^{2+}$ than that of $[Ni(AAPTMS)_2]^{2+}$.

Figure 9(c) and 9(d) show PAS's of Cu/APTMS/MCM-41 and Cu/AAPTMS/MCM-41, respectively. Only strong band at ca. 600nm, which is assigned to the spin allowed transtion $^2E_{2g} \rightarrow ^2T_{2g}$, indicates that both complexes are an octahedral geometry. It have been reported that absorption bands for a series of $[Cu(NH_3)_n(H_2O)_{6-n}]^{2+}$(n=0-4) move from ca. 800 nm to *ca.* 600 nm with the increase of value n due to a stronger ligand field of ammonia.[21] The band at 606 nm of λ_{max} for Cu/APTMS/MCM-41 can be attributable to the formation of $[Cu(APTMS)_2(H_2O)_2]^{2+}$. As shown in Figure 9(d), PAS of Cu/AAPTMS/MCM-41 shows a intensive and broad band of λ_{max} value at *ca.* 646 nm. Because of Jahn-Teller effect, it is expected that the Cu(II) in Cu/AAPTMS/MCM-41 is not coordinated by two AAPTMS's but by a AAPTMS and three water molecules. It is conformed by the slight

weakened intensity and the red shift of band of Cu/AAPTMS/MCM-41 comparing to that of Cu/APTMS/MCM-41.

Comparing to MCM-41, the PAS band shapes of complexes onto MCM-48 are similar to those of corresponding MCM-41 with the variation of PAS intensity. Though the atomic ratios of metal to silicon for most of MCM-48 based samples using EDX(KEVEX Corp. KEVEX superdry detector) are larger than those of MCM-41 as listed in Table 1, the PAS intensity decreased inversely in comparison with those of MCM-41 based samples, as shown in Figure 10 (a)-(f). It may be due to the adsorbed water molecules within MCM-48 samples. Exceptionally, PAS of Co/AAPTMS/MCM-48 shows higher intensity than that of Co/AAPTMS/MCM-41, which may be due to the increase of and a portion of tetrahedral complexes whose molar absorptivity is an order of magnitude higher than octahedral one.

Metal ions impregnated within MCM-41 and MCM-48 without immobilized aminosilane was removed completely upon stirring in water for 2 h at room temperature. On the
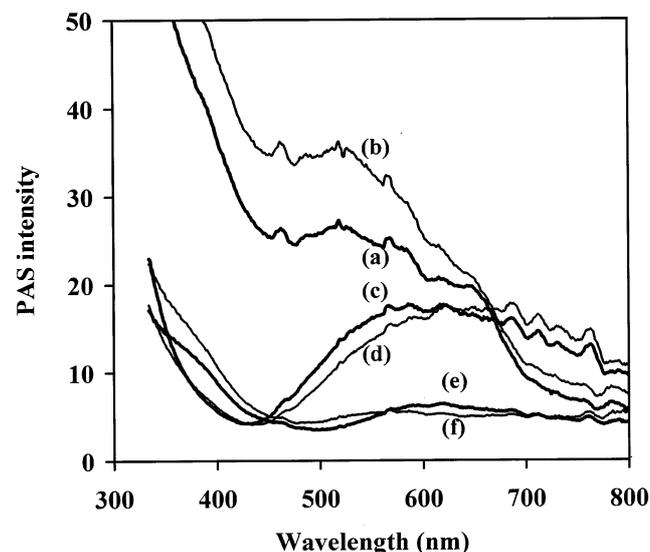

Figure 10. Photoacoustic spectra of (a) Co/APTMS/MCM-48, (b) Co/AAPTMS/MCM-48, (c) Cu/APTMS/MCM-48, (d) Cu/AAPTMS/MCM-48, (e) Ni/APTMS/MCM-48, and (f) Ni/AAPTMS/MCM-48.

contrary, metal ions coordinated by amminosilanes immobilized onto MCM-41 and MCM-48 were stable while treatment with water. This result reflect that most of metal ions are coordinated by ligating N atoms of aminosilanes without the impregnation on the surface of MCM-41.

References

1. Kresge, C. T.; Leonowicz, M. E.; Roth, W. J.; Vatuli, J. C.; Beck, J. S. *Nature* **1992**, *359*, 710.
2. Beck, J. S.; Vartuli, J. C.; Roth, W. J.; Leonowicz, M. E.; Kresge, C. T.; Schmitt, K. D.; Chu, C. T.-W.; Olson, D. H.; Sheppard, E. W.; McCullen, S. B.; Higgins, J. B.; Schlenker, J. L. *J. Am. Chem. Soc.* **1992**, *114*, 10834.
3. Maschmeyer, T.; Rey, F.; Sankar, G.; Thomas, J. M. *Nature* **1995**, *378*, 159.
4. Chen, C.-Y.; Li, H.-X.; Davis, M. E. *Microporous Mater.* **1993**, *2*, 17.
5. Liu, C.-J.; Li, S.-G.; Pang, W.-Q.; Che, C.-M. *Chem. Commun*. **1997**, 65.
6. Rao, Y. V. S.; Vos, D. E. D.; Bein, T.; Jacobs, P. A. *Chem. Commun.* **1997**, 335.
7. O'Brien, S.; Tudor, J.; Barlow, S.; Drewitt, M. J.; Heyes, S. T.; O'Hare, D. *Chem. Commun.* **1997**, 641.
8. Cheng, C.-F.; Park, D. H.; Klinowski, J. *J. Chem. Soc., Faraday Trans.* **1997**, *93(1)*, 193.
9. Kim, J. M.; Kim, S. K.; Ryoo, R. *Chem. Commun.* **1998,** 259.
10. Tanev, P. T.; Vlaev, L. T. *J. Colloid Interface Sci.* **1993,** *160*, 100.
11. Rosencwaig, A.; Gersho, A. *J. Appl. Phys.* **1976**, *47*, 64.
12. Park, D. H.; Lee, K. W.; Choe, S. J. *Bull. Korean Chem. Soc.* **1995**, *16*, 469.
13. Chen, J.; Li, Q,; Xu, R.; Xiao F. *Angew. Chem., Int. Ed. Engl.* **1995**, *34*, 2694.
14. Tanever, S. J.; Clark, J. H.; Gray, G. W.; Heath, P. A.; Macquarrie, D. *J. Chem. Commun.* **1997**, 1147.
15. Michels, J. J.; Dorsey, J. G. *Langmuir* **1990**, *6*, 414.
16. Cotton, F. A.; Goodgame, D. M. L.; Goodgame, M. *J. Am. Chem. Soc.* **1961**, *83*, 4690.
17. Anderson, J. H. Jr. *J. Catal.* **1973**, *28*, 76.
18. Cotton F. A.; Wilkenson, G. A. *Advanced Inorganic Chemistry*; Wiley-Interscience: New York, U. S. A., 1988; p 730.
19. Frost D. C.; McDowell, C. A.; Woolsey, I. S. *Mol. Phys.* **1974**, *27*, 1473.
20. Anderson, J. H. *J. Catal.* **1972**, *26*, 277.
21. Sano, M.; Maruo, T.; Masuda, Y.; Yamatera, H. *Inorg. Chem.* **1984**, *23*, 4466.